Separation and Purification Technology 191 (2018) 233–243

Contents lists available at ScienceDirect

Separation and Purification Technology

journal homepage: www.elsevier.com/locate/seppur

Application of visible light on copper-doped titanium dioxide catalyzing degradation of chlorophenols

Justin Chun-Te Lin[a], Khajornsak Sopajaree[b], Thidarat Jitjanesuwan[b,c], Ming-Chun Lu[c,*]

[a] Department of Environmental Engineering and Science, Feng Chia University, Taichung 40724, Taiwan
[b] Department of Environmental Engineering, Chiang Mai University, Chiangmai 50200, Thailand
[c] Department of Environmental Resources Management, Chia Nan University of Pharmacy and Science, Tainan 71710, Taiwan

ARTICLE INFO

Keywords:
TiO_2
2-Chlorophenol
Visible light active photocatalyst
Characterizations
Design of experiments

ABSTRACT

Chlorophenols are extensively used in the anthroposphere, and their fates in the atmosphere, hydrosphere, biosphere and lithosphere and their degradations under natural light of great interests. The homogeneous photocatalytic degradation of 2-chlorophenol (2-CP) in titanium dioxide suspensions containing copper ions or/and sulfates has been well examined. In this study, TiO_2 is directly doped with copper sulfate by a sol-gel method to promote its visible light activity (VLA) following a post-calcination step. The effects of three parameters of synthesis (calcination temperature, amounts of dopant and nitric acid) on 2-CP degradations were experimentally investigated using a three-factor, two-level factorial design in the first stage. Catalysts of the most significant synthetic parameters were further synthesized at five calcined temperatures and characterized in the second stage. 2-CP was completely removed using catalysts that were doped 0.21 mol.% $CuSO_4$ with 0.1 vol.% nitric acid and then calcined at 300 °C for 6 h. Morphological variations with doping amount are observed from scanning electron micrographs. XRD patterns demonstrated a transformation from amorphous to the anatase phase, with replacement of Ti^{4+} by Cu^{2+} in the crystal structure of TiO_2. UV–visible light diffuse reflectance spectra of the doped catalysts exhibited red-shifts, revealing their VLA. Surface areas, measured by the BET method, decreased as the calcination temperatures increased, and the pore sizes increased. Moreover, effect of three operational parameters, including: (del) initial concentration of 2-CP, initial pH and the photocatalyst dosage, under visible-light irradiation were investigated to simulate the scenarios of degradation in the natural and artificial conditions. Optimal operational parameters were obtained at a catalyst dosage of 3 $g{\cdot}dm^{-3}$, an initial 2-CP concentration of 20 ppm and a solution pH of 5.5. The pH_{zpc} of the undoped and $CuSO_4$-doped TiO_2 were determined to be 3.5 and 3.84.

1. Introduction

Chlorophenol compounds and their derivatives (CPs) are widely and frequently used in the anthroposphere, such as intermediates in the manufacturing of pharmaceuticals, synthetic dyes, petrochemicals, biocides, pains, textiles, leather products and wood preservatives. CPs are classified as refractory xenobiotics and known to be precursors of the highly toxic polychlorodibenzo-*p*-dioxins and polychlorodibenzofurans (PCDD/Fs) during the incineration of industrial wastes. The release of CPs either from petroleum refining effluents, residual pesticides and insecticides in the soils, or from degradation of complex chlorinated hydrocarbons among the atmosphere, hydrosphere, and lithosphere causes considerable environmental problems and ecological effects in the biosphere [1,2]. CPs not only cause unpleasant tastes and odors on drinking water but also cause oxidative stress. It is irritating to the skin, eyes, and damage the DNA of living organisms, as well as induce histopathological alterations, genotoxicity, mutagenicity and carcinogenicity in humans and animals. Consequently, their fates and aqueous environmental photochemistry are processes of great concerns [3,4]. 2-Chlorophenol (2-CP, or *ortho*-chlorophenol) is one of the toxic pollutants identified by the EU and US as priority contaminants [5]. Meanwhile, the monochlorophenol can be precursors of the higher-substituted CPs, and it is soluble in water (with a solubility of 28 $g{\cdot}L^{-1}$) at room temperature with a melting point of 9.3 °C) [6]. Consequently, it easily enters to aquatic ecosystems. Therefore, its transportation properties were addressed high concerns [7] as well as its toxicity and genotoxicity on bacteria, fish and human cells were recently re-evaluated [8].

Removal technologies of phenolic contaminants in the fluid streams were classified in two types as separation (such as distillation,

* Corresponding author.
E-mail address: mmclu@mail.cnu.edu.tw (M.-C. Lu).

http://dx.doi.org/10.1016/j.seppur.2017.09.027
Received 1 June 2017; Received in revised form 11 September 2017; Accepted 12 September 2017
Available online 19 September 2017
1383-5866/

extraction, adsorption, membranes-related processes) and destructive ones (such as supercritical, wet air, thermal and catalytic oxidations) [9,10]. Advanced oxidation processes (AOPs) [11], such as heterogeneous photocatalysis [12] and Fenton-like oxidation [13], were categorized to the destructive type and reported that can effectively remove CPs [14]. Titanium dioxide (TiO_2) is the most popular photocatalyst due to its highly stable chemical structure, relatively low cost, lack of toxicity, and photo-generation of highly oxidizing holes [15]. It is applied as one of the versatile AOPs. Commercial TiO_2 (Degussa P-25) has been intensively utilized to decompose 2-CP either irradiated by UV alone [16,17 or with concomitant UV (UV-A, -B, and -C) irradiation [18]. P-25 is also combined with adsorption (as with clay mineral) [19], with H_2O_2 [20], or with applied external bias voltage [21]. A TiO_2-UV suspension system with another semiconductor (CdS) efficiently degrades 2-CP [22]. Ga,I-co-doped TiO_2 was synthesized for photocatalytic degradation of 2-CP [23]. Nanoporous S-doped and N-doped TiO_2 were prepared to degrade 2-CP under LED irradiations [24,25. Except TiO_2, other nanoparticles like Cu-nano zeolite [26], ZnO [27], and ZrO_2-doped $ZnCo_2O_4$ [28] can remove 2-CP under irradiation by UV or visible light. Recently, cobalt oxide-loaded TiO_2, supported with reduced graphene oxide, was synthesized and applied to degrade 2-CP under visible light irradiation [29]. Table 1 compares the 2-CP photo-degradation efficiencies under various irradiation systems.

The function of copper ions in TiO_2 suspension as a homogeneous photocatalytic system has been well examined. The effects of dissolved transition metal ions (such as Cu^{2+}, Fe^{3+} and Ag^{+}) in several heterogeneous photocatalytic systems have been reviewed [30]. The effects of Cu^{2+} ions (from $CuCl_2$) on the formation of H_2O_2 from photocatalytic TiO_2 particles have also been investigated [31]. The effect of the charge trapping species, Cu^{2+} ions from $Cu(NO_3)_2$, on the photocatalytic oxidation of resorcinol was studied [32]. The surface and interfacial Cu^{2+} sites in CuO–TiO_2 nanocomposites improved their photoactivity [33]. The effect of adding small amounts of Cu^{2+} (from 0.001 to 0.8 $mmol{\cdot}L^{-1}$) in aqueous solution on photocatalytic degradation of methamidophos under UV irradiation has also been investigated [34]. Cu^{2+} behaves as an electron scavenger, described by Eq. (1). It prevented the recombination of electron–hole pairs, and increased the probability of the formation of ·OH and $\cdot O_2^-$ on the TiO_2 surface. However, the photodegradation efficiency decreased markedly as Cu^{2+} concentration increased above 0.006 $mmol{\cdot}L^{-1}$. This may be caused by the photogenerated holes on the surface of TiO_2 particles or ·OH, as presented in Eqs. (2) and (3):

$$Cu^{2+} + e^- \rightarrow Cu^{+} \quad (1)$$

$$Cu^{+} + h^{+} \rightarrow Cu^{2+} \quad (2)$$

$$Cu^{+} + \cdot OH + H^{+} \rightarrow Cu^{2+} + H_2O \quad (3)$$

Rate constants of phenol photodegradation with three types of TiO_2 (Degussa P25, TiO_2 of anatase and rutile phases from Sigma–Aldrich) under UV or visible-light irradiations in the presence of Cu^{2+} ions showed higher than those of the Cu^{2+}-absence solutions [35]. The co-addition of Cu^{2+} and F^- has been reported synergistically and significantly to improve the degradation rate constant of phenol relative to that obtained by adding one of the two ions [36]. The reversible photoreductive deposition and oxidative dissolution of Cu^{2+} in TiO_2 aqueous suspensions has also been reported [37]. The role of superoxide radicals in the catalyzing effects of adding copper ions on photo-oxidation in TiO_2 suspensions has been investigated [38]. Therefore, Cu^{2+} ions in solution considerably facilitate TiO_2 photocatalysis.

In contrast to homogeneous photocatalysis, copper ions can be directly incorporated into TiO_2 by various synthetic methods and formed a heterogeneous photocatalytic system. As the band-gap of pristine TiO_2 is rather large (3.0–3.2 eV), only a small fraction (about 5%) of the solar spectrum can be utilized. Researchers are making consistent efforts to improve the visible light activity (VLA) of TiO_2 [39]. Surface modification [40] and doping with either anions (such as nitrogen, sulfur, and halogen) or cations (such as rare earth, noble and transition metals) are popular approaches [41]. Cu-doped TiO_2 has been compared with N- and S-doped TiO_2, which are obtained by adding nitric or adding sulfuric acid, during sol-gel synthesis. The preparation in the presence of H_2SO_4 has been concluded by improving the photocatalytic activity [42]. To enhance photocatalytic activity of phenol degradation, CuP, CuO and CaO have been utilized as modifiers of TiO_2 [43], a cooperative effect between the cation (Cu^{2+}, acting as an electron scavenger) and the phosphate anion (acting as an organic adsorbent) in the dopant CuP has been reported. Cu-doped TiO_2 that is synthesized in a low temperature hydrolysis reaction reportedly has a very low band gap (1.6 eV) [44]. The linear and nonlinear optical properties of bare and Cu-doped TiO_2 prepared by the sol-gel method have been examined [45]. Liu et al. [46] synthesized Cu-doped TiO_2 via a conventional sol-gel method. UV–vis diffuse reflectance spectra (UV–vis DRS) of their Cu-doped TiO_2 that was prepared with various amounts of dopant exhibited considerable shifts of the peaks toward the visible range of approximately 400–800 nm. The demonstrated red-shift phenomena show the absorption bands extending to the visible or even the near-infrared range, favoring VLA. Cu-doped TiO_2 that is formed by wet-impregnation or the sol-gel method is popularly used in disinfection under either UVA [47] or visible light [48,49]. Cu-doped TiO_2 that is prepared by an incipient wetness impregnation method has been used continuously to photocatalytically degrade a gaseous contaminant [50]. 2-Propanol has been decomposed to CO_2 by acetone under visible light (> 400 nm) using Cu-grafted TiO_2 [51]. Recently, Cu-doped TiO_2 that had been prepared by a solvo-thermal method was utilized in the simultaneous photocatalytic reduction of CO_2 and the production of H_2, which may has the potential double benefits of reducing the carbon footprint of the generation of alternative energy source [52].

As co-doping TiO_2 with two or multiple elements cause promising results in the utilization of visible light, the use of these photocatalysts is attractive in terms of less energy required, safety hazardous and environmental impacts in comparing with utilising traditional UV irradiation source (e.g. mercury lamps). For example, triple-elemental doping (K, Al, S) with TiO_2 has been synthesized to oxidize efficiently 2-CP under illumination by visible light. It was found to exhibit higher photocatalytic performance than pristine or commercial TiO_2 [53]. Currently, $CuSO_4$-doped TiO_2 that had been prepared by a wet impregnation method was used in the selective catalytic reduction of NO by NH_3 [54]. $CuSO_4$-doped TiO_2 has been prepared by a single-step sol-gel method for the degradation of methyl orange in visible light [55]. Hence, in this work $CuSO_4$ is used as a multifunctional dopant in a sol-gel process to improve the VLA of TiO_2. The effects of three synthetic parameters of $CuSO_4$-doped TiO_2 on the degradation of 2-CP were investigated using a preliminary 2^3 factorial experimental design, and the degradation efficiencies were experimentally evaluated in fine-tuning parameters. The as-prepared catalysts were characterized by scanning electron microscopy (SEM), X-ray diffractometry (XRD), the Brunauer-Emmett-Teller (BET) method, UV–vis DRS and dynamic light scattering (DLS) to reveal their morphology, crystalline structure, surface and particle properties. The pH values at zero point charge of the pristine and $CuSO_4$-doped TiO_2 were determined. Three operational parameters of the photocatalytic degradation of 2-CP under simulated visible light irradiation (blue LEDs) were evaluated.

2. Experimental

2.1. Synthesis of catalysts

$CuSO_4$-doped TiO_2 catalysts were prepared using a popular sol-gel method, as shown into our previous study with some modifications [53]. A 0.05 mole amount of titanium butoxide ($Ti(OBu)_4$, 98%, Alfa Aesar) was firstly mixed with 70 mL analytical grade ethanol (EtOH, 99.5%, Merck) in a 250 mL flask with vigorous stirring at ambient temperature to yield a clear solution (Solution I). The flask was then

Table 1
Comparison of 2-CP photo-degradation efficiency under various systems.

Types of catalyst/sorbent	Irradiation light source	Dosages of catalyst/sorbent	pH (pH_{zpc})	2-CP (mg/L)	Removal efficiency	Ref.
TiO_2 (P25) suspension	UV (125 W)	0.1–6.0 × 10^{-3} kmol·m^{-3}	3–12	0.3–12.0	–	[16]
TiO_2 (P25) suspension	UV (400 W)	0.2 g·L^{-1}	5	100	95%	[17]
TiO_2 (P25) suspension	UV-A (along), UV-ABC (concomitant) 250 W	0.5 g·L^{-1}	4.2–4.5 (un-adjusted)	45 and 400 μM (adsorption)	99.8%	[18]
TiO_2 (P25) + H_2O_2	UV (15 W, λ = 254 nm; 250 W, λ = 315–400 nm)	0.1 g·L^{-1}, 0.3 g·L^{-1}, 0.5 g·L^{-1}.	pH_0 = 6.5, pH_f = 3.2, pH_f = 3.4, pH_f = 3.5	1 mM (18 mM of H_2O_2 if applied)	92% after 6 h (final), 75%, 67%, 60%	[20]
TiO_2 (P25) + external bias voltage + with various dissolved oxygen (D.O.) concentrations	UV (15 W, λ = 365 nm)	P25 was impregnated as TiO_2/Ti anode (containing with $NaClO_4$ served as electrolyte)	3, 7, 9	10	40% in D.O. conc. of 37.2 mg/L (oxygen bubbling); 50% in D.O. conc. of 0.5 mg/L (nitrogen bubbling).	[21]
TiO_2 (P25) + CdS suspension	UV (100 W)	each 0.5 g·L^{-1}	7.0	100	50% (TiO_2 amended), 87% (CdS amended), 100% (TiO_2 + CdS)	[22]
Chitosan/cobalt ferrite nanocomposite	Natural sunlight	100 mg·L^{-1}	3, 5, 7, 10	100	95.4%	[62]
TiO_2-In_2O_3 photocatalysts (sol-gel method)	High pressure Hg lamp (125 W), a cutoff filter (λ > 340 nm	2 g·L^{-1} (In_2O_3 and $TiCl_4$ were used as precursors, calcined at 200 °C and 500 °C)	–	10^{-3} mol·L^{-1}	The maximum removal of 2-CP at ca. 10 wt.% of In_2O_3	[63]
Co(III)-doped TiO_2	UV (100 W, λ = 228–420 nm)	10 mg·L^{-1}	9, 12	25	93.4%, 96.4%	[64]
N-doped mesoporous titania	UV (500 W) Natural sunlight	0.1%(w/v)	7	50	98.6%, 72.2%	[65]
Ga, I-co-doped TiO_2	Dysprosium lamp (400 W, similar to sunlight)	1.5 g	–	0.4 mM	89.3% (Max. achieved by 0.5%-Ga,I-TiO_2-400 °C) after 4 h	[23]
Ru-doped TiO_2	Visible light (λ = 254 nm), UV (6 W)	4 mg·L^{-1}	6	100	53%	[66]
ZrO_2-doped $ZnCo_2O_4$	Visible light (λ > 400 nm, 150 W)	1 g·L^{-1}	3, 5, 7	50	91.7%	[28]
S-doped TiO_2; Green irradiation (put in an ultrasonic 40 of kHz for 40 min)	Visible light (LED: λ = 490 nm, λ = 565 nm, λ = 660 nm)	1 g·L^{-1} (50 mg/50 mL)	2, 4, 6, 8, 10	25	71.4%, 71.5%, 86.7% (Max. at pH of 6 for λ = 660 nm, over 6 h)	[24]
N-doped TiO_2	Visible light (LED: λ = 490, 565, 660 nm)	1 g·L^{-1} (50 mg/50 mL)	2, 4, 6, 8, 10	25	79.8% (Max. at pH of 8 for λ = 660 nm, over 2.5 h)	[25]
TiO_2, TiO_2-RGO, TiO_2-CoO, TiO_2-RGO-CoO	Visible light (20–200 W)	0.5 g·L^{-1}	6	10	35.2%, 48.9%, 58.9%, 98.2%	[29]
Cu-nano zeolite	(adsorption only)	4 g·L^{-1}	2–10 (6.03)	50, 100, 200, 300, 240 (real wastewater)	81.8%	[26]
$CuSO_4$-doped TiO_2	Blue LED light (λ = 440–490 nm)	3 g·dm^{-3}	5.5 (3.84)	20	100%	This study

Note. The pH_0 and three pH_f respectively stand for pH value measured in the beginning (pH 6.5) and end of three experiments (pH = 3.2, 3.5 and 3.5), which using different dosages of 0.1, 0.3, and 0.5 g·L^{-1}.

placed in a water bath whose temperature was maintained at 4 °C. Meanwhile, 20 mL of deionized water (18.2 MΩ cm, produced by a Millipore system) was added to 20 mL of anhydrous EtOH with various amounts of copper sulfate (0.07, 0.14, 0.21, 0.28 and 0.35 mol.% $CuSO_4$), which was used as a multiple-element dopant. The mixture was continuously stirred until the doping element had completely dissolved (Solution II). The Solution II was dropwise added to Solution I, and precipitates were immediately formed. The mixed liquor of Solution I and II was continuously stirred for 1 h. Nitric acid (0.05 or 0.15 V/V), then added to control the rate of hydrolysis. The liquor was mixed 3 h into undergo hydrolytic condensation. The obtained hydrolyzed solution was then dried in an oven at 120 °C for 6 h and pulverized into a powder. The powder was calcined at 200 or 600 °C in a furnace for 10 h.

2.2. Experimental designs and set-up

In the first stage, experiments based on the 2^3 factorial designs (FD) were carried out by using statistical software (Minitab 17, Minitab Inc.). The simulations used two levels (−1 and +1) to represent the two extreme values of the three synthetic parameters (0.07 and 0.35 mol.% of dopant, calcined at 200 and 600 °C, with the addition of 0.05 and 0.15 v/v of nitric acid), as indicated in Table 2. The responses (Y), presented as percentage degradation of 2-CP using the catalysts that were synthesized under the above conditions, calculated from initial (C_0, ppm) and residual 2-CP concentrations (C_t, ppm) at sampling time *t*, as follows.

$$Y = (C_0 - C_t)/C_0 \times 100 \quad (4)$$

After comparing significance of the three synthetic parameters in the experimental design, the major significant one was calcination temperatures, which were further fine-tuning to calcine at five various temperatures (200, 300, 400, 500 and 600 °C). The samples synthesized in the second stage were named correspondingly as Ce200 to Ce600. The photocatalytic degradation experiments were conducted in a batch reactor, which included a 1-L Pyrex beaker equipped with a magnetic stirrer, pH meter, a thermometer and a water bath. The experiment set-up is schematically depicted as shown in Fig. 1, and temperature in the water bath was maintained at 25 °C. Five light emitting diode (LED, HR16 1W/110) lamps that emitted visible light in the wavelength range 440–490 nm were used as light sources 5 cm above the reactor. Three operational parameters were investigated and previous FD estimates were validated. 5 mL of the solution, which was sampled every two hours, was filtered through 0.2 mm GHP membranes with GHP 25 mm Acrodiscs syringe filters (Pall Co., USA). The degradations of 2-CP by the as-synthesized catalysts under visible light was monitored over 6 h by analyzing the concentration of the samples.

2.3. Methods of analysis and characterization

High-performance liquid chromatography (HPLC, Thermo Scientific) with an ODP-506D column (150 mm × 6 mm × 5 mm, Asahipak) and a Spectra SYSTEM model SN4000 pump (Showa Denko, Ltd., Tokyo, Japan) were carried out to determine concentrations of 2-CP. Standards were prepared from 0.2 to 1.0 ppm of 2-CP beforehand and scanned at a wavelength of 216 nm using a UV–visible detector. The coefficient of determination achieved (R^2 = 0.999) demonstrated the calibration curve was almost linear.

Scanning electron microscopy (QUANTA 200) at 10 kV was used to observe the morphology of the as-synthesized catalysts with various amounts of doping. X-ray diffraction (DX-2000 SSC) from 5° to 75° with a step size of 0.06° was used to elucidate the structural properties of the catalysts that have been calcined at various temperatures. A UV–visible spectrophotometer (U-3310, Hitachi) in diffuse reflectance mode was used to determine VLA of the TiO_2 catalysts. A surface area and porosimetry analyzer (ASAP 2010, Micromeritics) was used with the BET

Table 2
Designs of experiments for synthesis of $CuSO_4$-doped TiO_2.

Parameters		Unit	Levels	
			−1	+1
Amount of dopant (A)		mol.%	0.07	0.35
Calcination temperature (B)		°C	200	600
Amount of nitric acid (C)		v/v	0.05	0.15
Runs	A: amount of dopant (mol.%)	B: calcination Temperature (°C)	C: amount of nitric acid (V/V)	Y (%)
1	0.07	200	0.05	87.094
2	0.07	600	0.05	93.018
3	0.35	600	0.15	93.010
4	0.07	600	0.15	74.012
5	0.07	200	0.15	95.979
6	0.35	200	0.05	61.401
7	0.35	600	0.05	95.568
8	0.35	200	0.15	80.018

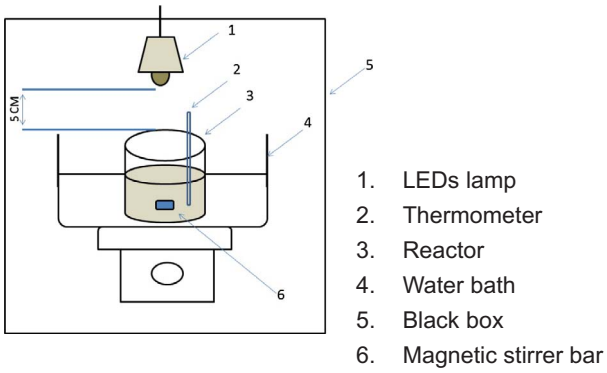

Fig. 1. Schematic diagram of the photocatalytic reactor.

method to determine the specific surface area of each catalyst. A dynamic light scattering particle analyzer (NanoBrook 90Plus Zeta, Brookhaven Instruments) was used to measure the distribution of sizes of the catalyst particles in suspension.

3. Results and discussion

3.1. Designs of experiments for synthesizing catalysts

The effects of three parameters of the synthesis of $CuSO_4$-doped TiO_2, i.e. (A) amount of dopant, (B) amount of acid added during sol-gel process, and (C) the calcination temperature on degradations, under visible light irradiation were preliminarily investigated by designs of experiments (DoE). Two extreme values as two levels (+1 and −1) for each of the three parameters was used in the DoE and the 2-CP removal percentages (% Y) were obtained in eight runs as indicated in Table 2. As shown in Fig. 2, increasing the calcination temperature (from 200 to 600 °C) and the volume of nitric acid (from 0.05 to 0.15 V/V) increased the percentage of 2-CP removed (from 81 to 89%, and from 84 to 86%, respectively), while increasing the amount of dopants (0.07–0.35 mol.% of $CuSO_4$) reduced it (from 87% to 82%). The volume of nitric acid showed less significant than the other two parameters. Accordingly, the first two parameters (A and B) were the main focus in the following syntheses, and an average amount (0.1 v/v) of nitric acid was fixed thereafter. Insights concerning the two synthetic parameters were gained by applying fine-tuning effects of the parameter A (0.07, 0.14, 0.21, 0.28 to 0.35 mol.%) and B (200, 300, 400, 500 and 600 °C) within the initially estimated two values in the DoE.

3.2. Effects of synthetic parameters

Two control experiments that involved only visible light irradiation (without a catalyst) and only the dopant $CuSO_4$ (as dark adsorption) were performed. Their results were compared with those obtained with photocatalysis using the $CuSO_4$-doped TiO_2. As presented in Fig. 3(a), direct photolysis of the solution that contained 2-CP by irradiation degraded limited amounts in the 7 h experiment while dark adsorption in the solution that contained homogeneous $CuSO_4$ removed only 10% of 2-CP. The $CuSO_4$ dissolved as a cation (Cu^{2+}) and an anion (SO_4^{2-}) and redox reactions such as Eq. (1) proceeded to degrade 2-CP without TiO_2 to 23%. In contrast, a significant proportion of phenol was removed when the solution using the $CuSO_4$-doped TiO_2 and illuminated by the visible light. The degradation of 2-CP with the as-prepared photocatalyst was complete by the 6th h. As a result, subsequent degradation experiments were all carried out for six hours.

Fig. 3(b) displays the effect of the amount of $CuSO_4$ dopant on the degradation of 2-CP with an initial concentration of 20 ppm at pH 5.5 and 40 °C. The degradation efficiency increased with the amount of dopant which is increased from 0.07 to 0.21 mol.%. However, further increasing amount of dopant (0.28 and 0.35 mol.%) did not increase the degradation of 2-CP. Doping at 0.21 mol.% yielded the highest degradation (98.92%) at the 6th h. Therefore, the average of these two amounts of dopant was used thereafter. Copper is known to be presented on the surface of TiO_2 as Cu^{2+} and Cu^{+}, and it can act as an electron trap through the following reactions. Since $CuSO_4$ contains two elements (Cu and S) that can work together in the electron-hole pair recombination, leaving the photogenerated holes to react with water molecules, forming hydroxyl radicals (˙OH), which in turn react with 2-CP and degrade them. Consequently, the rate of degradation of 2-CP is increased by the acceleration of interfacial charge transfer, as Cu^{+} can provide its trapped electrons to the adsorbed oxygen species. Similarly, doped sulfur can trap electrons, improving the photocatalytic activity of TiO_2. When O═S═O species are placed in water, S═O bonds become polarized and coordinate with water, inducing the electron-deficient sulfur species to act as an electron trap [55].

Based on the previous DoE, calcination temperature was identified as the most important synthetic parameter in the degradation of 2-CP. Therefore, gels of $CuSO_4$-doped TiO_2 (0.21 mol.%) were calcined at five temperatures for 1 h and the effect of temperature was examined in details. As shown in Fig. 3(c), the best degradation efficiency of 2-CP was obtained at 300 °C and complete removal (100%) was achieved by the 6th h. The degradation achieved using the catalyst calcined at 200 °C was 17% lower than that achieved using the catalyst calcined at 300 °C, and a higher calcination temperature (400, 500 and 600 °C) was

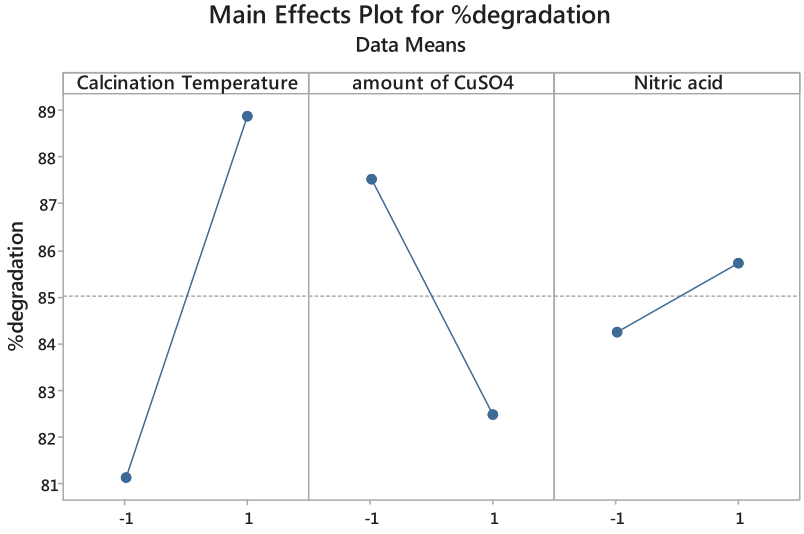

Fig. 2. Effects of three synthetic parameters on the degradations of 2-CP.

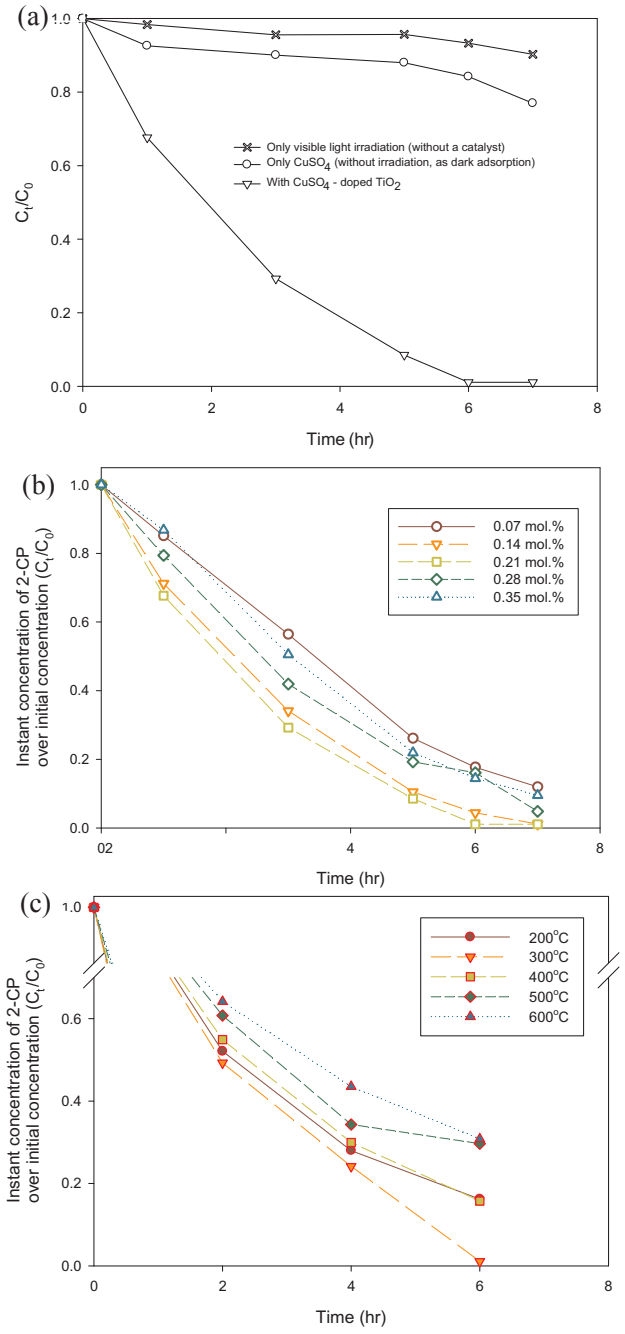

Fig. 3. (a) Removal of 2-CP under visible light irradiation only, with $CuSO_4$ only and with $CuSO_4$-doped TiO_2 under visible light irradiation; Effect of (b) $CuSO_4$ doping amounts and (c) calcination temperatures on photocatalytic degradation under visible light irradiation (initial concentration of 2-CP: 20 ppm, at pH 5.5 and 40 °C).

associated with lower degradation efficiency (84.3, 70.2 and 69.2%). In summary, 2-CP was effectively degraded by using the VLA photocatalysts that were doped 0.21 mol.% $CuSO_4$ with 0.1 vol.% nitric acid and then calcined at 300 °C for 6 h.

3.3. Characterizations of the $CuSO_4$-doped TiO_2

The morphologies of the TiO_2 doped with various amounts of $CuSO_4$ and calcined at 300 °C for 6 h were elucidated by SEM, as displayed in Fig. 4. Irregularly shaped particles were observed on the surfaces of the catalysts. A more rugged surface and smaller particles were observed

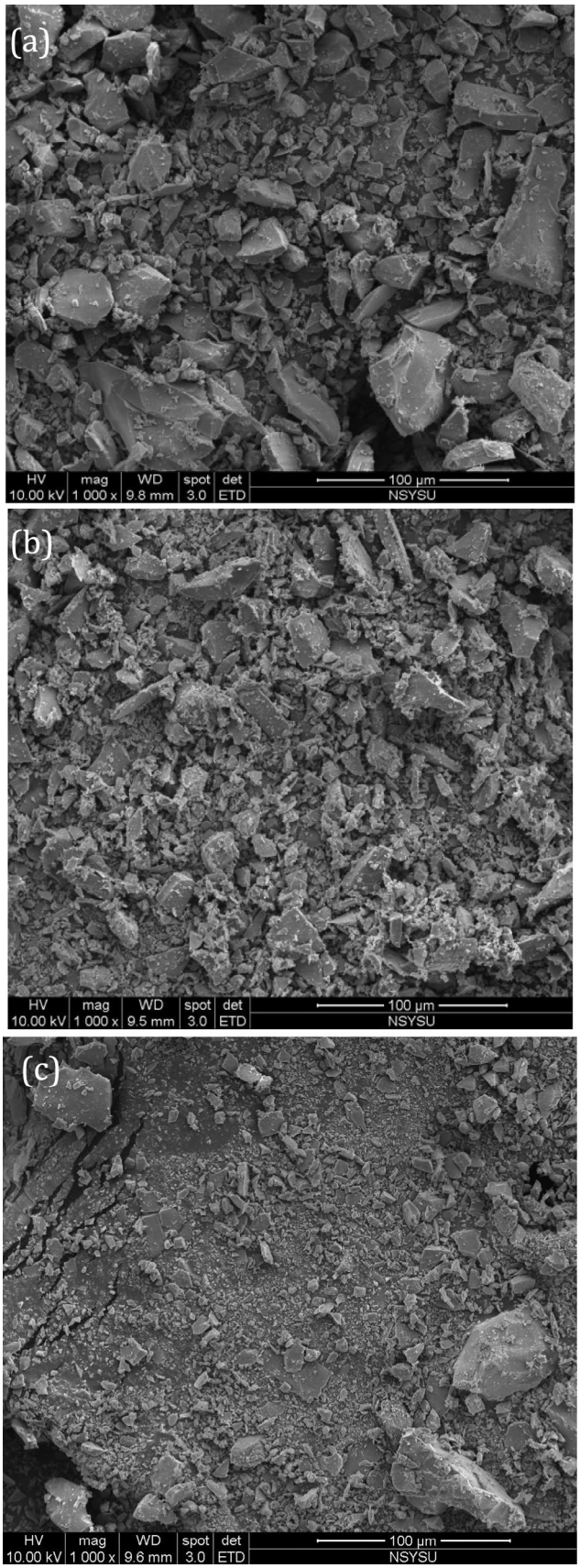

Fig. 4. Scanning electron micrographs of TiO_2 doped with various amounts of $CuSO_4$: (a) 0.07, (b) 0.21, (c) 0.35 mol.%; all calcined at 300 °C for 6 h.

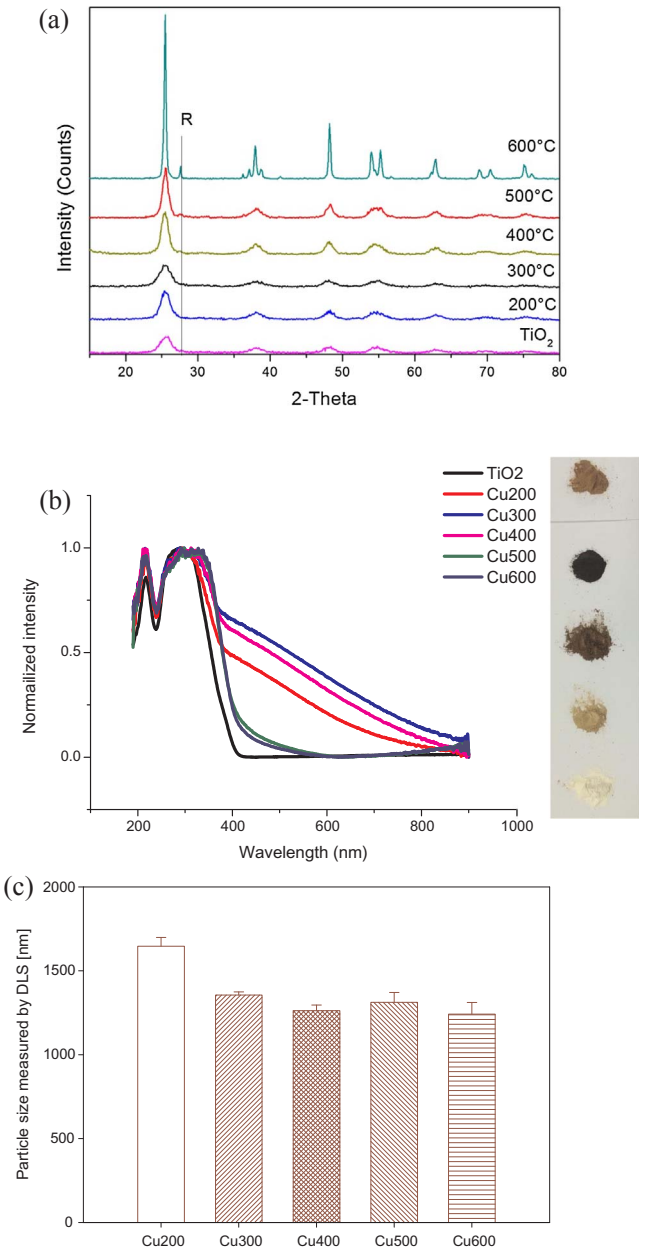

Fig. 5. Characterizations of pristine TiO_2 and $CuSO_4$-doped TiO_2 calcined at various temperatures (from 300 to 600 °C): (a) XRD patterns (A and R respectively representing the crystal plane of anatase and rutile), (b) UV–visible diffusive reflectance spectrum (photo of five samples from top to bottom are Cu200, Cu300, Cu400, Cu500, Cu600), and (c) particle size in aqueous suspensions measured by dynamic light scattering.

when the amount of $CuSO_4$ had increased from 0.07 to 0.35 mol.%, as displayed in Fig. 4(a)–(c). More active sites were thought to have been formed for the smaller particles on the synthesized TiO_2 when large amounts of dopant were used. The degradation of 2-CP as maximized by a doping of 0.21 mol.%, and the morphology in Fig. 4(b) proves that this amount of doping yielded particles of optimal size for photocatalysis.

Since calcination temperature of $CuSO_4$-doped TiO_2 was the dominant synthetic parameter, the structures and physicochemical properties of the as-synthesized catalysts were characterized by XRD, the BET method, UV–vis DRS and DLS. Firstly, XRD analysis of the pristine and $CuSO_4$-doped TiO_2 calcined at various temperatures was used to identify their constituent phases and to calculate their crystallite sizes. As presented at the bottom of Fig. 5(a), no distinct pattern was obtained from the pristine TiO_2, which was therefore identified as amorphous. As the calcination temperature increased from 200 to 600 °C, transformation from the amorphous to the anatase phase occurred as Ti^{4+} was replaced by Cu^{2+} in the crystal structure of TiO_2. The crystallite sizes of the five $CuSO_4$-doped TiO_2 were calculated using Scherrer's equation, as described elsewhere [53], increasing from 9.67, through 10.5, 8.86, 9.90 and 11.98 nm as the calcination temperature increased as specified. The sizes were similar to those of other Cu-doped TiO_2 prepared by the same sol-gel method with the addition of 0.5 and 1.0 mol.% nitric or sulfuric acid, but using different copper and titanium precursors [42], the crystallite sizes of the undoped, Cu-N or Cu-S codoped TiO_2 (from 10 to 38 nm) all increased with calcination temperature from 400 to 700 °C. The XRD pattern of Cu-doped TiO_2 that had been calcined at 500 °C [34] included four peaks at 25°, 38°, 48°, and 54°, which revealed an anatase phase of TiO_2. Gonell et al. [52] showed the difference between the XRD patterns of Cu-doped TiO_2 before and after calcination at 500 °C, where the crystallite size increased from 6.4–6.9 nm to 12.9–14.1 nm. These crystallite sizes calculated as using XRD were generally consistent with the results herein. The literature also includes XRD characterizations of $CuSO_4$-doped TiO_2. Yadav et al. [48] obtained XRS patterns at ~25.45° from the same precursor of $CuSO_4$ of 1.0–3.0 mol.% that had been prepared by sol-gel synthesis and calcined at 500 °C for 5 h. Recently, Yu et al. [54] prepared $CuSO_4$-doped TiO_2 by a wet impregnation method and preheating TiO_2 at 300 °C for 3 h, adding $CuSO_4$ (1, 2 and 4 wt.%) to solution and calcining at 500 °C for 5 h. Although the obtained diffraction peaks were very close to those obtained herein, no crystallite size was calculated. Whereas the XRD patterns herein revealed the evolutions of the photocatalyst structures at various calcination temperatures, XRD patterns of $CuSO_4$-doped TiO_2 [57], which had almost the same constituents as those herein, but was calcined at 450 °C only, varied with the amount of dopant. Since the ionic radius of sulfate substantially exceeds those of Cu^{2+} (0.073 nm) and Ti^{4+} (0.068 nm), the cation is more easily incorporated into the matrix as a substituent of TiO_2 without causing much crystalline distortion.

The UV–visible DRS of as-synthesized catalysts was scanned from 200 to 900 nm, as presented in Fig. 5(b). A broad intense absorption band at 380 nm was a result of charge transfer from the valence band (mainly formed from the 2 p orbital of O^{2-}) to the conduction band (mainly formed from the 3d t_{2g} orbital of Ti^{4+}). Strong red-shifts (toward to the visible light range of approximately 400 to 700 nm) were obtained from for $CuSO_4$-doped TiO_2 calcined at 300, 400 and 200 °C, while calcination at higher temperatures (500 and 600 °C) slightly improved VLA about that of pristine TiO_2. The red-shift in the UV–vis DRS was recently reported to increase with the amount of $CuSO_4$ (5, 2 and 0 wt.%) dopant [57]. Notably, the preparation of TiO_2 in the presence of nitric acid (either 0.5 or 1.0 mol.%) [42] clearly accelerates surface utilization and the calculated band-gap energy declines (from 3.33 to 3.06 eV) as the calcination temperature increase (from 400, through 500 to 600 °C). A minimal concentration of Cu^{2+} dopant in the host lattice of TiO_2 forms oxygen vacancies due to the charge compensation effect shifting the optical absorption of Cu–doped TiO_2 and extending into the visible light region (Sahu and Biswas, 2011).

Surface areas, pore volumes (V_P) and pore sizes (r_A), of the five catalysts calcined at various temperatures were measured, and shown in Table 3. The surface areas of $CuSO_4$-doped TiO_2 measured which were using the BET method (S_{BET}) decreased (from 278.4, through 271.8, 218.7, and 158.2 to 117.3 $m^2 \cdot g^{-1}$) as the calcination temperature increased (from 200, through 300, 400, and 500 to 600 °C) for 1 h. Hence the pore size (r_A) increased consequently (from 27.6, through 31.2, 39.8, and 48.9 to 57.8 Å). Surface areas that were measured using other methods (Langmuir, t-plot external and single point) followed the same trends as those measured using the BET method. Similarly, the S_{BET} of Cu-doped TiO_2 dramatically decreasing from 123, 11 to 1 $m^2 \cdot g^{-1}$ and from 117, 21 to < 1 $m^2 \cdot g^{-1}$, as the calcination temperature (from 400, to 500 to 600 °C for 2 h) when 0.5 and 1.0 mol.% of Cu $(NO_3)_2$, respectively, were added as a copper precursor in the presence

Table 3
BET results of $CuSO_4$-doped TiO_2 at calcination temperatures of 200–600 °C.

Sample name	Surface area [unit: m^2/g]				Pore volume [unit: cm^3/g]	Pore size [unit: Å]
	BET	Langmuir	t-Plot external	Single point	Single point adsorption total pore volume of pores	Adsorption average pore width (4 V/A by BET)
Cu200	278.4	393.5	317.0	258.5	0.192317	27.6
Cu300	271.8	384.8	310.7	253.4	0.211779	31.2
Cu400	218.7	307.0	240.9	206.6	0.217801	39.8
Cu500	158.2	221.2	172.3	150.2	0.193308	48.9
Cu600	122.7	170.2	129.7	117.3	0.177311	57.8

of nitric acid [42]. However, the S_{BET} of sulfated titania catalysts doped with various amounts (0, 2, 5 and 10 wt.%) of copper (Cu^{2+}-SO_4^{2-}-TiO_2) varied less consistently (70, 85, 110 and 73 $m^2 \cdot g^{-1}$). The S_{BET} of $CuSO_4$-TiO_2 catalysts prepared by a wet impregnation method [54] decreased (from 56.6, through 54.3, and 54.0 to 52.9 $m^2 \cdot g^{-1}$) as the amount of $CuSO_4$ increased (from 0, through 1, and 2 to 4 wt.%).

The variation of color with calcination temperature is visible even to the naked eyes, as seen in the right part of Fig. 5(b). Following calcination at the highest temperature (600 °C), the photocatalyst was white, changing to yellow, brown and black as the temperatures was reduced (at 500, 400 and 300 °C, respectively). During calcination, the crystallization of TiO_2 was simultaneous with the removal of residual organic compounds. However, incomplete thermal decomposition of the organic matter may have occurred at 200 °C, producing the brown color. These results suggest that the effects of calcination temperature may be visible. As displayed in Fig. 5(c), the particle sizes of the five forms of $CuSO_4$-doped TiO_2 in aqueous suspension were measured using DLS. The lowest calcination temperature (200 °C) yielded the largest particles (1646.6 ± 52.4 nm), and higher calcination temperatures (300–600 °C) were associated with smaller particles (1241 ± 70.0–1355.8 ± 18.7 nm).

3.4. Degradation scenarios

The effects of pH, temperature, initial concentration, dose of catalyst and oxygen concentration on the degradation of CP have been reviewed [14]. Also, parameters of the influencing heterogeneous photocatalytic degradation of phenolic contaminants in wastewater have been reviewed [12]. A batch UV-LED reactor was used to degrade photocatalytically phenol by Degussa P25 TiO_2 [58]. In this study, three principal parameters that influence the degradation efficiencies of the as-prepared catalysts were examined using a batch reactor with five blue LED lamps as the visible light source. As presented in Fig. 6(a), the effect of initial concentration from 10 to 50 ppm on 2-CP degradation was investigated. The initial concentration clearly affected photocatalytic degradation, and both 20 and 10 ppm yielded 100% removal by the 6th h. The effect of initial concentration in the range of 0.1–6 × 10^{-3} $kmol \cdot m^{-3}$ on the degradation of 2-CP by commercial TiO_2 (Degussa P25) under UV irradiation has been examined [16], yielding the same trend as obtained herein for $CuSO_4$-doped TiO_2. Fig. 6(b) plots the effect of photocatalyst dosage on the 2-CP degradation efficiency. The use of 3 g of the as-prepared photocatalyst in visible light yielded the optimal result, and 2 g dosage removed almost all 2-CP by the 6th h. A lower dosage of the catalyst (1 g) could not provide enough activate sites for photocatalysis, so its rate of degradation was lower than those achieved by using 2 and 3 g. Agglomeration (particle-particle interaction) and sedimentation occurred at the higher dosages of catalyst (4 and 5 g) so the excess particles in the system reduced the available surface area for photon absorption.

As displayed in Fig. 6(c), the effect of initial pH on the 2-CP degradation efficiency generally showed declined over time. Initial acidic conditions favored the degradation of 2-CP in visible light, the highest efficiency was obtained at pH 5.5 and the increased acidity (pH 2 and 3) did not facilitate the degradation. A set of experimental data reported elsewhere [20] can be a reference with our data. The more P25 TiO_2 added (0, 0.1, 0.3 and 0.5 $g \cdot L^{-1}$), the more pH drop (from the initial value of 6.5 respectively decrease to 3.0, 3.2, 3.4 and 3.5) under UV irradiation (at wavelength of 254 nm) over the same period (6-h) could be obtained. Although higher mineralization was obtained with a higher dosage of added TiO_2 in that study [20], the 2-CP removal was decreased. Therefore, consistently maintaining solution pH is critical. A higher rate constant for the direct UV photolysis of 2-CP was obtained under more alkaline conditions (as determined at pH values of 3, 5, 7 and 11) and without a Pyrex filter (eliminating light radiation with $\lambda < 300$ nm) at neutral pH [6]. The effect of solution pH (from 3 to 12) on the degradation of 2-CP by commercial TiO_2 (Degussa P25) under UV irradiation has been investigated [16], and the rate constant was found to be lower in an acid medium than in a basic medium. Doong et al. [22] also considered the effect of pH (from 2.5 to 12.5) on the photocatalytic degradation of 2-CP in TiO_2 suspensions, and found that fewer aromatic intermediates were formed at higher pH, which suggested photodegradation at high pH favors direct ring cleavage.

The aggregation of TiO_2 particles occurs as the conditioning pH approaches pH_{zpc}, as it tends to stabilize at either higher or lower pH conditions [56].

For a positively charged surface, $pH<pH_{zpc}$: $TiO_2 + nH^+ \leftrightarrow TiO_2H_n^{+n}$ (5)

For a negatively charged surface, $pH>pH_{zpc}$: $TiO_2 + nOH^- \leftrightarrow TiO_2(OH)_n^{-n}$ (6)

Owing to the amphoteric nature of the surface hydroxyl groups, metal oxides (such as TiO_2) are used as diprotic acids. The surface titanol group of ($> Ti\text{-}OH_2^+$) undergoes the following acid-base equilibrium reaction [40]:

$$>Ti-OH_2^+ \leftrightarrow > Ti-OH + H^+ pK_{a1} \quad (7)$$

$$>Ti-OH \leftrightarrow > TiO^- + H^+ pK_{a2} \quad (8)$$

The average pK_a corresponds to the points of zero charge (pH_{zpc}) as shown below.

$$pK_a = \frac{pK_{a1} + pK_{a2}}{2} = pK_{zpc} \quad (9)$$

pH_{zpc} can be determined either by measuring the electrophoretic mobility of suspended particles as a function of pH (zeta potential) or by using a mass titration method [59]. The latter approach is utilized herein, as presented in Fig. 6(d), and pH_{zpc} values of $CuSO_4$-doped and undoped TiO_2 of 3.84 and 3.5, respectively, are obtained. The pH_{zpc} of the undoped TiO_2 is consistent with our previously measured value (3.51) [53], and the pH_{zpc} of TiO_2 doped with 0.21 mol.% $CuSO_4$ in this study was slightly higher (3.84) than the values (3.39, 2.37 and 1.90) for TiO_2 doped with a larger amount (0.2–1.0 mol.%) of another sulfate dopant, $KAl(SO_4)_2$. As stated in various studies [56,60], the pH_{zpc} of commercial TiO_2 is approximately pH 6.3–6.85, which is close to the theoretical value obtained from Eq. (9) and pK_{a1} and pK_{a2} of Degussa P25 are 4.5 and 8, respectively. Kosmulski updated the pH-dependent surface charge and the pH_{zpc} [61], which can serve as references in determining the optimal pH for either homogeneous or heterogeneous photocatalysis systems. Tu et al. [10] prepared three catalysts from municipal sewage sludge and used in the catalytic wet air oxidation of 2-CP. The measured pH_{zpc} of the pyrolysis sludge derived carbons, supported with iron oxide, and washing afterwards were respectively 7.5, 4.2 and 3.7, which were interesting to compare as a reference here.

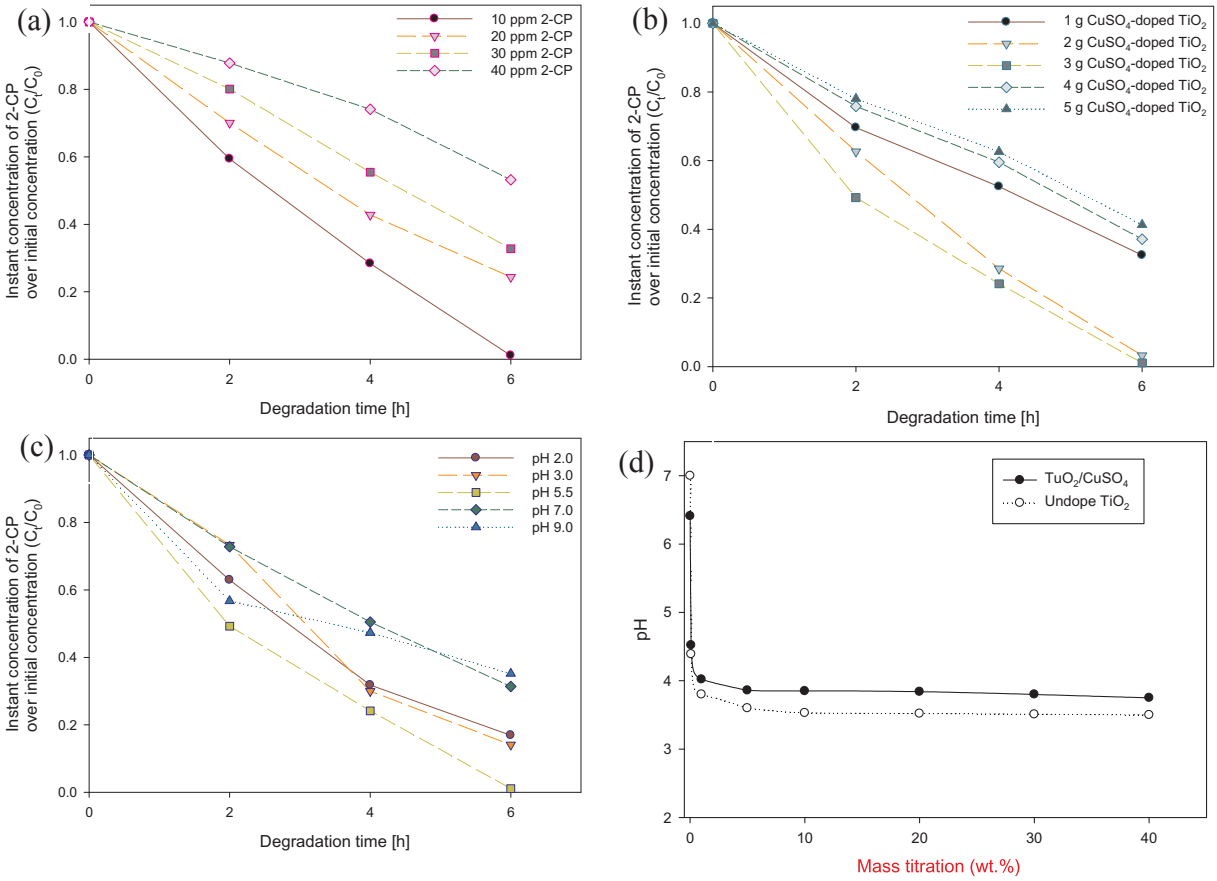

Fig. 6. Effect of (a) initial concentration of 2-CP, (b) photocatalyst dosage, (c) initial pH on photocatalytic degradation under visible light irradiation (conditions were kept at 20 ppm 2-CP, pH 5.5 and 40 °C if not specifically noted); (d) The pH_{zpc} of synthesized TiO_2 catalyst as determined using mass titration.

4. Conclusion

This study has established that $CuSO_4$-doped TiO_2 can be an effective VLA photocatalyst of the degradation of 2-chlorophenol, which is one of the toxic pollutants that is also a priority contaminants. The three-factor, two-level factorial design preliminarily scans three synthetic parameters (calcination temperature, amounts of dopant and nitric acid) in the first stage. Catalysts of the most significant synthetic parameters were further synthesized at five calcined temperatures and characterized in the second stage. The most effective VLA TiO_2 catalyst was doped with 0.21 mol.% using 0.1 v/v of nitric acid and then calcined at 300 °C for 6 h. Morphologies with three amounts of dopants were observed SEM, and XRD patterns revealed the effects of calcination temperature on the crystalline structures of the catalysts. Crystallite sizes in the range 9.67–11.98 nm were calculated. Red-shifts of the UV–visible DRS of catalysts that were calcined between 200 and 400 °C on proved revealed a shift of the absorption spectrum toward the visible-light region, so the as-synthesized photocatalysts can be applied in the treatment of wastewater that contains refractory phenolic compounds. Moreover, surface areas determined by the BET method and particle sizes in the aqueous suspensions measured by DLS all provided information about structural properties and the effects of calcination temperatures thereon. The photocatalysts were most effective at a dosage of 3 $g \cdot dm^{-3}$, with an initial 2-CP concentration of 20 ppm and a solution pH of 5.5. The pH_{zpc} values of undoped and $CuSO_4$-doped TiO_2 were determined as 3.5 and 3.84.

Acknowledgments

The authors would like to thank the National Science Council, Taiwan (NSC 99-2221-E-041-012-MY3) for their support through funding this research. UV-vis DRS for measuring VLA of the catalysts, which was kindly supported by Prof. Chih-Hsien Chen, Department Chemical Engineering in FCU, and DLS for measuring particle size in aqueous suspensions, which was kindly supported by Prof. Kou-Bin Cheng, Textile and Material Industry Research Center in FCU, were both acknowledged.

Appendix A. Supplementary material

Supplementary data associated with this article can be found, in the online version, at http://dx.doi.org/10.1016/j.seppur.2017.09.027.

References

[1] E.O. Igbinosa, E.E. Odjadjare, V.N. Chigor, I.H. Igbinosa, A.O. Emoghene, F.O. Ekhaise, N.O. Igiehon, O.G. Idemudia, Toxicological profile of chlorophenols and their derivatives in the environment: the public health perspective, Sci. World J. (2013) 1–11, http://dx.doi.org/10.1155/2013/460215 (Article ID 460215).
[2] T. Faludi, C. Balogh, Z. Serfőző, I. Molnár-Perl, Analysis of phenolic compounds in the dissolved and suspended phases of Lake Balaton water by gas chromatography-tandem mass spectrometry, Environ. Sci. Pollu. Res. 22 (2015) 11966–11974, http://dx.doi.org/10.1007/s11356-015-4734-x.
[3] M. Czaplicka, Sources and transformations of chlorophenols in the natural environment, Sci. Total Environ. 322 (2004) 21–39, http://dx.doi.org/10.1021/jp307240u.
[4] S. Rayne, K. Forest, K.J. Friesen, Mechanistic aspects regarding the direct aqueous environmental photochemistry of phenol and its simple halogenated derivatives. A review, Environ. Int. 35 (2009) 425–437, http://dx.doi.org/10.1016/j.envint.2008.09.004.
[5] Agency for Toxic Substances and Disease Registry (ATSDR), Priority List of Hazardous Substances, The ATSDR 2015 Substance Priority List, U.S. Department of Health and Human Services, Public Health Service, Atlanta, GA, 2015. <http://www.atsdr.cdc.gov/spl/> (assessed 19.09.07).
[6] M. Czaplicka, Photo-degradation of chlorophenols in the aqueous solution, J. Hazard. Mater. B 134 (2006) 45–59, http://dx.doi.org/10.1016/j.jhazmat.2005.10.039.

[7] L.F.G. Martins, M. Cristina, B. Parreira, J.P. Prates Ramalho, P. Morgado, E.J.M. Filipe, Prediction of diffusion coefficients of chlorophenols in water by computer simulation, Fluid Phase Equilibr. 396 (2015) 9–19, http://dx.doi.org/10.1016/j.fluid.2015.03.026.

[8] D. Vlastos, M. Antonopoulou, I. Konstantinou, Evaluation of toxicity and genotoxicity of 2-chlorophenol on bacteria, fish and human cells, Sci. Total Environ. 551–552 (2016) 649–655, http://dx.doi.org/10.1016/j.scitotenv.2016.02.043.

[9] G. Busca, S. Berardinelli, C. Resini, L. Arrighi, Technologies for the removal of phenol from fluid streams: a short review of recent developments, J. Hazard. Mater. 160 (2008), http://dx.doi.org/10.1016/j.jhazmat.2008.03.045.

[10] Y. Tu, Y. Xiong, S. Tian, L. Kong, C. Descormea, Catalytic wet air oxidation of 2-chlorophenol over sewagesludge-derived carbon-based catalysts, J. Hazard. Mater. 276 (2014) 88–96, http://dx.doi.org/10.1016/j.jhazmat.2014.05.024.

[11] R. Andreozzi, V. Caprio, A. Insola, R. Marotta, Advanced oxidation processes (AOP) for water purification and recovery, Catal. Today 53 (1999) 51–59, http://dx.doi.org/10.1016/S0920-5861(99)00102-9.

[12] S. Ahmed, M.G. Rasul, R. Brown, M.A. Hashib, Influence of parameters on the heterogeneous photocatalytic degradation of pesticides and phenolic contaminants in wastewater: a short review, J. Environ. Manage. 92 (2011) 311–330, http://dx.doi.org/10.1016/j.jenvman.2010.08.028.

[13] H.H. Huang, M.C. Lu, J.N. Chen, Catalytic decomposition of hydrogen peroxide and 2-chlorophenol with iron oxides, Water Res. 35 (2001) 2291–2299, http://dx.doi.org/10.1016/S0043-1354(00)00496-6.

[14] M. Pera-Titus, V. García-Molina, M.A. Baños, J. Giménez, S. Esplugas, Degradation of chlorophenols by means of advanced oxidation processes: a general review, Appl. Catal. B Environ. 47 (2004) 219–256, http://dx.doi.org/10.1016/j.apcatb.2003.09.010.

[15] A. Fujishima, T.N. Rao, D.A. Tryk, Titanium dioxide photocatalysis, J. Photochem. Photobiol. C 1 (2000) 1–21, http://dx.doi.org/10.1016/S1389-5567(00)00002-2.

[16] L. Rideh, A. Wehrer, D. Ronze, A. Zoulalian, Photocatalytic degradation of 2-chlorophenol in TiO_2 aqueous suspension: modeling of reaction rate, Ind. Eng. Chem. Res. 36 (1997) 4712–4718, http://dx.doi.org/10.1021/ie0203274.

[17] N.N. Rao, A.K. Dubey, S. Mohanty, P. Khare, R. Jain, S.N. Kaul, Photocatalytic degradation of 2-chlorophenol: a study of kinetics, intermediates and biodegradability, J. Hazard. Mater. B101 (2003) 301–314, http://dx.doi.org/10.1016/S0304-3894(03)00180-8.

[18] G. Li Puma, P.L. Yue, Effect of the radiation wavelength on the rate of photocatalytic oxidation of organic pollutants, Ind. Eng. Chem. Res. 41 (2002) 5594–5600, http://dx.doi.org/10.1021/ie0203274.

[19] I. Ilisz, A. Dombi, K. Mogyorósi, A. Farkas, I. Dékány, Removal of 2-chlorophenol from water by adsorption combined with TiO_2 photocatalysis, Appl. Catal. B Environ. 9 (2002) 247–256, http://dx.doi.org/10.1155/2013/460215.

[20] M. Bertelli, E. Selli, Reaction paths and efficiency of photocatalysis on TiO_2 and of H_2O_2 photolysis in the degradation of 2-chlorophenol, J. Hazard. Mater. 138 (2006) 46–52, http://dx.doi.org/10.1016/j.jhazmat.2006.05.030.

[21] Y. Ku, Y.C. Lee, W.Y. Wang, Photocatalytic decomposition of 2-chlorophenol in aqueous solution by UV/TiO_2 process with applied external bias voltage, J. Hazard. Mater. 138 (2006) 350–356, http://dx.doi.org/10.1016/j.jhazmat.2006.05.057.

[22] R.A. Doong, C.H. Chen, R.A. Maithreepala, S.M. Chang, The influence of pH and cadmium sulfide on the photocatalytic degradation of 2-chlorophenol in titanium dioxide suspensions, Water Res. 35 (2001) 2873–2880, http://dx.doi.org/10.1016/S0043-1354(00)00580-7.

[23] S. Song, C. Wang, F. Hong, Z. He, Q. Cai, J. Chen, Gallium- and iodine-co-doped titanium dioxide for photocatalytic degradation of 2-chlorophenol in aqueous solution: role of gallium, Appl. Surf. Sci. 257 (2011) 3427–3432, http://dx.doi.org/10.1016/j.apsusc.2010.11.040.

[24] N. Sharotri, D. Sud, A greener approach to synthesize visible light responsive nanoporous S-doped TiO_2 with enhanced photocatalytic activity, New J. Chem. 39 (2015) 2217–2223, http://dx.doi.org/10.1039/c4nj01422g.

[25] N. Sharotri, D. Sud, Ultrasound-assisted synthesis and characterization of visible light responsive nitrogen-doped TiO_2 nanomaterials for removal of 2-Chlorophenol, Desal. Water Treat. 57 (2016) 8776–8788, http://dx.doi.org/10.1080/19443994.2015.1026278.

[26] P.T. Huong, B.K. Lee, J. Kim, Improved removal of 2-chlorophenol by a synthesized Cu-nano zeolite, Process Safe. Environ. 100 (2016) 272–280, http://dx.doi.org/10.1016/j.psep.2016.02.002.

[27] J. Rashid, M.A. Barakat, N. Salah, S.S. Habib, ZnO-nanoparticles thin films synthesized by RF sputtering for photocatalytic degradation of 2-chlorophenol in synthetic wastewater, J. Ind. Eng. Chem. 23 (2015) 134–139, http://dx.doi.org/10.1016/j.jiec.2014.08.006.

[28] J. Rashid, M.A. Barakat, R.M. Mohamed, I.A. Ibrahim, Enhancement of photocatalytic activity of zinc/cobalt spinel oxides by doping with ZrO_2 for visible light photocatalytic degradation of 2-chlorophenol in wastewater, J. Photochem. Photobiol. A Chem. 284 (2014) 1–7, http://dx.doi.org/10.1016/j.jcis.2007.03.007.

[29] A. Sharma, B.K. Lee, Rapid photo-degradation of 2-chlorophenol under visible light irradiation using cobalt oxide-loaded TiO_2/reduced graphene oxide nanocomposite from aqueous media, J. Environ. Manage. 165 (2016) 1–10, http://dx.doi.org/10.1016/j.jenvman.2015.09.013.

[30] M.I. Litter, Heterogeneous photocatalysis transition mental ions in photocatalytic systems, Appl. Catal. B Environ. 23 (1999) 89–114, http://dx.doi.org/10.1016/S0926-3373(99)00069-7.

[31] R. Cai, Y. Kubota, A. Fujishima, Effect of copper ions on the formation of hydrogen peroxide from photocatalytic titanium dioxide particles, J. Catal. 219 (2003) 214–218.

[32] S.W. Lam, K. Chiang, T.M. Lim, R. Amal, G.K.C. Low, Effect of charge trapping species of cupric ions on the photocatalytic oxidation of resorcinol, Appl. Catal. B Environ. 55 (2005) 123–132, http://dx.doi.org/10.1016/j.apcatb.2004.08.004.

[33] G. Li, N.M. Dimitrijevic, L. Chen, T. Rajh, K.A. Gray, Role of surface/interfacial Cu^{2+} sites in the photocatalytic activity of coupled CuO–TiO_2 nanocomposites, J. Phys. Chem. C 112 (2008) 19040–19044, http://dx.doi.org/10.1021/jp8068392.

[34] C. Liu, J. Wang, W. Chen, C. Dong, C. Li, The removal of DON derived from algae cells by Cu-doped TiO_2 under sunlight irradiation, Chem. Eng. J. 280 (2015) 588–596, http://dx.doi.org/10.1016/j.cej.2015.05.113.

[35] L. Wan, J. Sheng, H. Chen, Y. Xu, Different recycle behavior of Cu^{2+} and Fe^{3+} ions for phenol photodegradation over TiO_2 and WO_3, J. Hazard. Mater. 262 (2013) 114–120, http://dx.doi.org/10.1016/j.jhazmat.2013.08.002.

[36] N. Wang, Z. Chen, L. Zhu, X. Jiang, B. Lv, H. Tang, Synergistic effects of cupric and fluoride ions on photocatalytic degradation of phenol, J. Photochem. Photobio. A 191 (2007) 193–200, http://dx.doi.org/10.1016/j.jphotochem.2007.04.023.

[37] N.S. Foster, R.D. Noble, C.A. Koval, Reversible photoreductive deposition and oxidative dissolution of copper ions in titanium dioxide in aqueous suspensions, Environ. Sci. Technol. 27 (1993) 350–356, http://dx.doi.org/10.1021/es00039a016.

[38] Y. Dua, S. Goldstein, J. Rabani, The catalytic effects of copper ions on photo-oxidation in TiO_2 suspensions: the role of superoxide radicals, J. Photochem. Photobio. A 225 (2011) 1–7, http://dx.doi.org/10.1016/j.jphotochem.2011.07.004.

[39] S. Rehman, R. Ullah, A.M. Butt, N.D. Gohar, Strategies of making TiO_2 and ZnO visible light active, J. Hazard. Mater. 170 (2009) 560–569, http://dx.doi.org/10.1016/j.jhazmat.2009.05.064.

[40] H. Park, Y. Park, W. Kim, W. Choi, Surface modification of TiO_2 photocatalyst for environmental applications, J. Photochem. Photobiol. C 15 (2013) 1–20, http://dx.doi.org/10.1021/ie0203274.

[41] A. Zaleska, Doped-TiO2: a review (1872-2121/08 $100.00 + .00), Recent Pat. Eng. 2 (2008) 157–164.

[42] G. Colón, M. Maicu, M.C. Hidalgo, J.A. Navió, Cu-doped TiO_2 systems with improved photocatalytic activity, Appl. Catal. B 67 (2006) 41–51, http://dx.doi.org/10.1016/j.apcatb.2006.03.019.

[43] H. Chen, Y. Xu, Cooperative effect between cation and anion of copper phosphate on the photocatalytic activity of TiO_2 for phenol degradation in aqueous suspension, J. Phys. Chem. C 116 (2012) 24582–24589, http://dx.doi.org/10.1021/jp307240u.

[44] T. Aguilar, J. Navas, R. Alcántara, C. Fernández-Lorenzo, J.J. Gallardo, G. Blanco, J. Martín-Calleja, A route for the synthesis of Cu-doped TiO_2 nanoparticles with a very low band gap, Chem. Phys. Lett. 457 (2013) 202–205, http://dx.doi.org/10.1016/j.cplett.2013.04.007.

[45] B. Rajamannan, S. Mugundan, G. Viruthagiri, P. Praveen, N. Shanmugam, Linear and nonlinear optical studies of bare and copper doped TiO_2 nanoparticles via sol gel technique, Spectrochim. Acta A Mol. Biomol. 118 (2014) 651–656, http://dx.doi.org/10.1016/j.saa.2013.09.045.

[46] W. Liu, S. Chen, W. Zhao, S. Zhang, Titanium dioxide mediated photocatalytic degradation of methamidophos in aqueous phase, J. Hazard. Mater. 164 (2009) 154–160, http://dx.doi.org/10.1016/j.jhazmat.2008.07.140.

[47] M. Khraisheh, L. Wu, A.H. Al-Muhtaseb, M.A. Al-Ghouti, Photocatalytic disinfection of Escherichia coli using TiO_2 P25 and Cu-doped TiO_2, J. Ind. Eng. Chem. 23 (2015) 134–139, http://dx.doi.org/10.1016/j.jiec.2015.02.023.

[48] H.M. Yadav, S.V. Otari, V.B. Koli, S.S. Mali, C.K. Hong, S.H. Pawar, S.D. Delekar, Preparation and characterization of copper-doped anatase TiO_2 nanoparticles with visible light photocatalytic antibacterial activity, J. Photochem. Photobiol. A 280 (2014) 32–38, http://dx.doi.org/10.1016/j.jphotochem.2014.02.006.

[49] C. Karunakaran, G. Abiramasundari, P. Gomathisankar, G. Manikandan, V. Anandi, Cu-doped TiO_2 nanoparticles for photocatalytic disinfection of bacteria under visible light, J. Colloid Interf. Sci. 352 (2010) 68–74, http://dx.doi.org/10.1016/j.jcis.2010.08.012.

[50] J. Araña, A. Peña Alonso, J.M. Doña Rodríguez, J.A. Herrera Melián, O. González Díaz, J. Pérez Peña, Comparative study of MTBE photocatalytic degradation with TiO_2 and Cu-TiO_2, Appl. Catal. B Environ. 78 (2008) 355–363, http://dx.doi.org/10.1016/j.apcatb.2007.09.023.

[51] H. Irie, S. Miura, K. Kamiya, K. Hashimoto, Efficient visible light-sensitive photocatalysts: grafting Cu(II) ions onto TiO_2 and WO_3 photocatalysts, Chem. Phys. Lett. 457 (2008) 202–205, http://dx.doi.org/10.1016/j.cplett.2008.04.006.

[52] F. Gonell, A.V. Puga, B. Julián-López, H. García, A. Corma, Copper-doped titania photocatalysts for simultaneous reduction of CO_2 and production of H_2 from aqueous sulfide, Appl. Catal. B Environ. 180 (2016) 263–270, http://dx.doi.org/10.1016/j.apcatb.2015.06.019.

[53] N.C. Tolosa, M.C. Lu, H.D. Mendoza, A.P. Rollon, The effect of the composition of tri-elemental doping (K, Al, S) on the photocatalytic performance of synthesized TiO_2 nanoparticles in oxidizing 2-chlorophenol over visible light illumination, Appl. Catal. A Gen. 401 (2011) 233–238, http://dx.doi.org/10.1016/j.apcata.2011.05.028.

[54] Y. Yu, J. Chen, J. Wang, Y. Chen, Performances of $CuSO_4$/TiO_2 catalysts in selective catalytic reduction of NO*x* by NH_3, Chin. J. Catal. 37 (2016) 281–287, http://dx.doi.org/10.1016/S1872-2067(15)60993-7.

[55] S. Livraghi, M.C. Paganini, E. Giamello, EPR study of electron trapping on partially hydroxylated alkali-earth oxides occurring during SO_2 disproportionation, J. Mol. Catal. A: Chem. 349 (2011) 100–104, http://dx.doi.org/10.1016/j.molcata.2011.08.004.

[56] R.A. French, A.R. Jacobson, B. Kim, S.L. Isley, R.L. Penn, P.C. Baveye, Influence of ionic strength, pH, and cation valence on aggregation kinetics of titanium dioxide nanoparticles, Environ. Sci. Technol. 43 (2009) 1354–1359, http://dx.doi.org/10.1021/es00039a016.

[57] R.D. Chekuri, S.R. Tirukkovalluri, One step synthesis and characterization of copper doped sulfated titania and its enhanced photocatalytic activity in visible light by

degradation of methyl orange, Chin. J. Chem. Eng. 24 (2016) 475–483, http://dx.doi.org/10.1016/S0021-9517(03)00197-0.
[58] A. Jamal, R. Vanraes, P. Hanselaer, T. van Gerven, A batch LED reactor for the photocatalytic degradation of phenol, Chem. Eng. Process. 71 (2013) 43–45, http://dx.doi.org/10.1016/j.cep.2013.03.010.
[59] J.P. Reymond, F. Kolenda, Estimation of the point of zero charge of simple and mixed oxides by mass titration, Powder Technol. 103 (1999) 30–36, http://dx.doi.org/10.1016/S0032-5910(99)00011-X.
[60] C.E. Hsiung, H.L. Lien, A.E. Galliano, C.S. Yeh, Y.H. Shih, Effects of water chemistry on the destabilization and sedimentation of commercial TiO_2 nanoparticles: Role of double-layer compression and charge neutralization, Chemosphere 151 (2016) 145–151, http://dx.doi.org/10.1021/es00039a016.
[61] M. Kosmulski, The pH-dependent surface charging and points of zero charge: V Update, J. Colloid Interf. Sci 353 (2011) 1–15, http://dx.doi.org/10.1016/j.jcis.2014.02.036.
[62] F. Manal, A. Taleb, Adsorption and photocatalytic degradation of 2-CP in waste water onto CS/$CoFe_2O_4$ nanocomposite synthesized using gamma radiation, Carbohyd. Polym. 114 (2014) 65–72, http://dx.doi.org/10.1016/j.carbpol.2014.07.061.
[63] D. Shchukin, S. Poznyak, A. Kulak, P. Pichat, TiO_2-In_2O_3 photocatalysts: Preparation, characterisations and activity for 2-CP degradation in water, J. Photochem. Photobiol. A 162 (2004) 423–430, http://dx.doi.org/10.1016/S1010-6030(03)00386-1.
[64] M.A. Barakat, H. Schaeffer, G. Hayes, S. Ismat-Shah, Photocatalytic degradation of 2-chlorophenol by Co-doped TiO_2 nanoparticles, Appl. Catal. B Environ. 57 (2005) 23–30, http://dx.doi.org/10.1016/j.apcatb.2004.10.001.
[65] P.A. Mangrulkar, S.P. Kamble, M.M. Joshi, J.S. Meshram, N.K. Labhsetwar, S.S. Rayalu 1, , Photocatalytic degradation of phenolics by N-doped mesoporous titania under solar radiation, Int. J. Photoenergy (2012) 10, http://dx.doi.org/10.1155/2012/780562 (Article ID 780562).
[66] R.A. Elsalamony, S.A. Mahmoud, Preparation of nanostructured ruthenium doped titania for the photocatalytic degradation of 2-chlorophenol under visible light, Arab. J. Chem. 10 (2017) 194–205, http://dx.doi.org/10.1016/j.arabjc.2012.06.008.